Global Change Biology

Weakened growth of cropland N2O emissions in China associated with nationwide policy interventions

Journal:	*Global Change Biology*
Manuscript ID	Draft
Wiley - Manuscript type:	Primary Research Articles
Date Submitted by the Author:	n/a
Complete List of Authors:	Shang, Ziyin; Peking University, Sino-France Institute of Earth Systems Science, Laboratory for Earth Surface Processes, College of Urban and Environmental Sciences; University of Aberdeen, Institute of Biological and Environmental Science Zhou, Feng; Peking University, Ecology Smith, Pete; University of Aberdeen, Institute of Biological and Environmental Science Saikawa, Eri ; Emory University, Department of Environmental Sciences Ciais, Philippe; Laboratory for Climate Sciences and the Environment (LSCE) CHANG, Jinfeng; Laboratory for Climate Sciences and the Environment (LSCE) Tian, Hanqin; Auburn University, School of Forestry and Wildlife Sciences Del Grosso, Stephen J; USDA ARS, Soil Management and Sugar Beet Research Ito, Akihiko; National Institute for Environmental Studies, Center for Global Environmental Research Chen, Minpeng; Renmin University of China, School of Agricultural Economics and Rural Development Wang, Qihui; Peking University, Sino-France Institute of Earth Systems Science, Laboratory for Earth Surface Processes, College of Urban and Environmental Sciences BO, YAN; Peking University Cui, Xiaoqing; Peking University, Sino-France Institute of Earth Systems Science, Laboratory for Earth Surface Processes, College of Urban and Environmental Sciences Castaldi, Simona; Universita degli Studi della Campania Luigi Vanvitelli, Dipartimento di Scienze e Tecnologie Ambientali Biologiche e Farmaceutiche Juszczak, Radoslaw; Poznan University of Life Sciences, Department of Meteorology Kasimir, Åsa; University of Gothenburg, Department of Earth Sciences Magliulo, Vincenzo; National Research Council of Italy, Institute for Mediterranean Agriculture and Forest Systems Medinets, Sergiy; Odessa National I. I. Mechnikov University, Regional Centre for Integrated Environmental Monitoring and Ecological Studies Medinets, Volodymyr; Odessa National I.I. Mechnikov University, Regional Centre for Integrated Environmental Monitoring and Ecological Studies Rees, Bob; Scotland's Rural College

	Wohlfahrt, Georg; University of Innsbruck, Institute of Ecology Sabbatini, Simone; University of Tuscia, DIBAF
Keywords:	Nitrous oxide, agricultural soils, emission inventory, flux upscaling, agricultural management, process-based model, temporal trend, spatial pattern
Abstract:	China has experienced rapid agricultural development over recent decades, accompanied by increased fertilizer consumption in croplands, yet the trend and drivers of the associated nitrous oxide (N2O) emissions remain uncertain. The primary sources of this uncertainty are the coarse spatial variation of activity data and the incomplete model representation of N2O emissions in response to agricultural management. Here we provide new data-driven estimates of cropland N2O emissions across China in 1990-2014, compiled using a global cropland-N2O flux observation dataset, nationwide survey-based reconstruction of N-fertilization and irrigation, and an updated nonlinear model. In addition, we have evaluated the drivers behind changing cropland N2O patterns using an index decomposition analysis approach. We find that China's annual cropland-N2O emissions increased on average by 11.2 Gg N yr□2 ($P < 0.001$) from 1990 to 2003, after which emissions plateaued until 2014 (2.8 Gg N yr□2, $P = 0.02$), consistent with the output from an ensemble of process-based terrestrial biosphere models (TBMs). The slowdown of the increase in cropland-N2O emissions after 2003 was pervasive across two thirds of China's sowing areas. This change was mainly driven by the nationwide reduction of N-fertilizer applied per area, partially due to the prevalence of the Nationwide Soil Testing and Formulation Fertilization Program that was launched in the early 2000s. This reduction has almost offset the N2O emissions induced by policy-driven expansion of sowing areas, particularly in the Northeast Plain and the lower Yangtze River Basin. Our results underline the importance of high-resolution activity data and adoption of nonlinear model of N2O emission for capturing cropland-N2O emission changes. Improving the representation of policy interventions is also recommended for future projections.

Weakened growth of cropland N_2O emissions in China associated with nationwide policy interventions

Ziyin Shang[1, 2], Feng Zhou[1]*, Pete Smith[2], Eri Saikawa[3], Philippe Ciais[4], Jinfeng Chang[4], Hanqin Tian[5], Stephen J. Del Grosso[6], Akihiko Ito[7], Minpeng Chen[8], Qihui Wang[1], Yan Bo[1], Xiaoqing Cui[1], Simona Castaldi[9], Radoslaw Juszczak[10], Åsa Kasimir[11], Enzo Magliulo[12], Sergiy Medinets[13], Volodymyr Medinets[13], Robert M. Rees[14], Georg Wohlfahrt[15], Simone Sabbatini[16]

[1]Sino-France Institute of Earth Systems Science, Laboratory for Earth Surface Processes, College of Urban and Environmental Sciences, Peking University, Beijing, 100871, P.R. China.
[2]Institute of Biological and Environmental Sciences, University of Aberdeen, 23 St Machar Drive, Aberdeen AB24 3UU, UK.
[3]Department of Environmental Sciences, Emory University, Atlanta, Georgia 30322, USA.
[4]Laboratoire des Sciences du Climat et de l'Environnement, CEA CNRS UVSQ, 91191 Gif-sur-Yvette, France
[5]International Center for Climate and Global Change Research, School of Forestry and Wildlife Sciences, Auburn University, Auburn, Alabama, USA
[6]Soil Management and Sugar Beet Research, USDA Agricultural Research Service, 2150 Centre Ave., Fort Collins, CO 80526, USA
[7]Center for Global Environmental Research, National Institute for Environmental Studies, Tsukuba, Japan
[8]School of Agricultural Economics and Rural Development, Renmin University of China, Beijing, 100872, P.R. China.
[9]Dipartimento di Scienze e Tecnologie Ambientali Biologiche e Farmaceutiche, Università degli Studi della Campania "Luigi Vanvitelli", via Vivaldi 43, 81100 Caserta, Italy.
[10]Department of Meteorology, Poznan University of Life Sciences, 60-649 Poznan, Poland.
[11]Department of Earth Sciences, University of Gothenburg, Gothenburg, Sweden.
[12]13I SAFOM-CNR, Institute for Mediterranean Agricultural and Forest Systems, National Research Council, Via Patacca 85, 80056 Ercolano (NA), Italy
[13]Regional Centre for Integrated Environmental Monitoring and Ecological Researches, Odessa National I. I. Mechnikov University (ONU), Mayakovskogo Lane 7, 65082 Odessa, Ukraine.
[14]Scotland's Rural College (SRUC), Edinburgh EH9 3JG, Scotland, UK.
[15]Institute of Ecology, University of Innsbruck, Sternwartestrasse 15, Innsbruck, Austria.
[16]Department for Innovation in Biological, Agro-food and Forest Systems (DIBAF), University of Tuscia, via S. Camillo de Lellis s.n.c., 01100 Viterbo, Italy.

***Corresponding Author**
Phone: +86 10 62756511, Fax: +86 10 62756560; Email: zhouf@pku.edu.cn.

ABSTRACT

China has experienced rapid agricultural development over recent decades, accompanied by increased fertilizer consumption in croplands, yet the trend and drivers of the associated nitrous oxide (N_2O) emissions remain uncertain. The primary sources of this uncertainty are the coarse spatial variation of activity data and the incomplete model representation of N_2O emissions in response to agricultural management. Here we provide new data-driven estimates of cropland N_2O emissions across China in 1990-2014, compiled using a global cropland-N_2O flux observation dataset, nationwide survey-based reconstruction of N-fertilization and irrigation, and an updated nonlinear model. In addition, we have evaluated the drivers behind changing cropland N_2O patterns using an index decomposition analysis approach. We find that China's annual cropland-N_2O emissions increased on average by 11.2 Gg N yr^{-2} ($P < 0.001$) from 1990 to 2003, after which emissions plateaued until 2014 (2.8 Gg N yr^{-2}, $P = 0.02$), consistent with the output from an ensemble of process-based terrestrial biosphere models (TBMs). The slowdown of the increase in cropland-N_2O emissions after 2003 was pervasive across two thirds of China's sowing areas. This change was mainly driven by the nationwide reduction of N-fertilizer applied per area, partially due to the prevalence of the Nationwide Soil Testing and Formulation Fertilization Program that was launched in the early 2000s. This reduction has almost offset the N_2O emissions induced by policy-driven expansion of sowing areas, particularly in the Northeast Plain and the lower Yangtze River Basin. Our results underline the importance of high-resolution activity data and adoption of nonlinear model of N_2O emission for capturing cropland-N_2O emission changes. Improving the representation of policy interventions is also recommended for future projections.

Keywords: Nitrous oxide; agricultural soils; emission inventory; flux upscaling; agricultural management; process-based model; temporal trend; spatial pattern

1. Introduction

Nitrous oxide (N_2O) is a potent greenhouse gas, with a global warming potential 265~298 times greater than that of CO_2 over a 100-year time horizon (Myhre et al., 2013). Its emissions are recognized as the most important ozone-depleting substance (Ravishankara, Daniel, & Portmann, 2009). Accumulating evidence points to croplands as the largest global source (>40%) of anthropogenic N_2O (Paustian et al., 2016). Global cropland N_2O emissions are projected to increase by ~50% from 2010 to 2050, due to the future intensification and expansion of cropland production (Alexandratos & Bruinsma, 2012). Reducing cropland N_2O emissions is a key mitigation option for limiting climate warming, especially in relation to recently developed policy objectives relating to climate change and concerns regarding ozone depletion (Allen et al. 2018). However, high spatial and temporal variability makes the estimation of cropland N_2O emissions notoriously difficult (e.g., quantity, pattern, trend) (Paustian et al., 2016), resulting in large discrepancies between bottom-up and top-down approaches (Tian et al., 2016).

One of the sources of uncertainty is the model structure of bottom-up approaches that consider a linear response of N_2O emissions to N application rate, as recommended in the Tier 1 method for a national N_2O inventory by the Intergovernmental Panel on Climate Change (IPCC, 2006). Recent synthesis of field observations suggests that N_2O emissions respond nonlinearly to an increasing N application rate (Philibert, Loyce, & Makowski, 2012; Shcherbak, Millar, & Robertson, 2014; Song et al. 2018) This nonlinear response was partially ascribed to the fact that high ammonium ion concentrations from urea hydrolysis inhibits nitrite transformation to nitrate (Ma, Shan, & Yan, 2015), resulting in nitrite accumulation which is subsequently emitted as N_2O. Philibert et al. (2012) proposed a nonlinear model with fixed parameters, which improved the predictive performance of N_2O flux. This model was further improved by using

86 random parameters from a more recent and a larger field observation dataset of N_2O flux
87 (Gerber et al., 2016). In addition to the nonlinear response of emissions to N inputs,
88 microbially-mediated N_2O is also strongly dependent on climate and soil properties (Perlman,
89 Hijmans, & Horwath, 2014). A spatially-referenced nonlinear model was therefore developed
90 to simulate N_2O emissions in response to fertilizer N application rate (N_{rate}) under various
91 environmental or management-related conditions (Zhou et al., 2015). Comparison between
92 models showed that such models outperformed nonlinear models with fixed or random
93 parameters (Zhou et al., 2015).
94
95 The accuracy of simulating N_2O emissions is dependent on the representation of model
96 parameters and the spatial aggregation of agricultural activity data. For example, a spatially-
97 referenced nonlinear model (Zhou et al., 2015) calibrated against observations in China was
98 able to better capture the variations of N_2O emissions on sites with similar conditions to the
99 calibration dataset, but was unable to reproduce emissions at other sites. To improve the
100 performance of diagnostic models at a regional scale, field observations representative of a
101 wide range of environmental and management-related variables are required. In addition, N_2O
102 emission models are sensitive to the degree of spatial aggregation in fertilizer and irrigation
103 data. Uncertainty of input data is expected to increase with decreasing spatial scale without
104 altering spatial differences in fertilizer and irrigation applications (Gerber et al., 2016).
105 Although the spatial resolution of management-related data is improving, mainly by evenly
106 disaggregating national-scale data into gridded maps (Lu & Tian, 2017; Zhang et al., 2017),
107 long-term, high-resolution maps of cropland-specific N-fertilizers and irrigation inputs are not
108 yet available at the global or regional scale.
109
110 China is currently the largest emitters of anthropogenic N_2O emissions globally (Zhou et al.,

111 2014). Over the past decades, this source in China increased with N-fertilizer use, accounting
112 for over 20% of global cropland-N_2O emissions from IPCC Tier 1 inventories (FAO, 2018;
113 Janssens-Maenhout et al., 2019; Winiwarter, Höglund-Isaksson, Klimont, Schöpp, & Amann,
114 2018). China is a large country with contrasting crop production systems, climate and soil types,
115 where the patterns of N_2O emissions are poorly understood compared to some developed
116 countries (Zou et al., 2010; Zhou et al., 2015; Yue et al., 2018). In the last decade, process-
117 based models (e.g., DNDC, DAYCENT, DLEM), used to produce Tier 3 IPCC estimates,
118 simulated global and regional cropland-N_2O emissions using sub-national N inputs from China
119 (Li et al, 2001; Tian et al., 2019; Yue et al., 2019). These models are arguably more realistic
120 than the Tier 1 approach because they account for climatic and soil variabilities. Although
121 multi-model ensemble may reduce some errors across individual models through a broader
122 integration of model processes (Tian et al., 2019), these individual models have rarely been
123 validated by observations across contrasting environmental and management-related
124 conditions (Ehrhardt et al., 2017), leading to large uncertainties not only in estimating emission
125 trends, but also in identifying underlying drivers.
126
127 To address these knowledge gaps, we re-estimate the spatial pattern and temporal trend of
128 cropland N_2O emissions across China in 1990-2014. We advance the estimation of spatially-
129 explicit, long-term cropland N_2O emissions in China by using an updated version of the
130 spatially-referenced nonlinear model (Zhou et al., 2015) with high-resolution, crop-specific
131 gridded datasets of N-fertilizer and irrigation uses. First, the model was updated through re-
132 calibration with N_2O emission observations three times more than previous dataset. Second,
133 maps (1-km) of crop-specific N-fertilization and irrigation application rates across Chin were
134 collated, based on a compilation of sub-national statistics or surveys (Zhou et al., 2014; Zou et
135 al. 2018), which differ from previous datasets based on downscaling of national totals (Lu &

Tian, 2017; Janssens-Maenhout et al., 2017) or modeling (Flörke, Schneider, & McDonald, 2018). Finally, using one type of index decomposition analysis (Ang, 2015), we separated the contributions of agricultural management practices and environmental conditions on cropland N_2O emission trends. This study considers direct emissions from croplands where synthetic fertilizers, livestock manure, human excreta, and crop residues are added, as well as indirect emissions due to atmospheric N deposition. Indirect emissions due to N leaching or runoff are not considered.

2. Data and methods

2.1 Updated spatially-referenced nonlinear model (SRNM)

The previous version of the SRNM model (Zhou et al., 2015) assume a quadratic relationship between cropland N application rates and N_2O emissions, with spatially-variable model parameters depending on climate, soil properties, and crop management practices. The SRNM predict cropland-N_2O emissions for each of geographical grids rather than administrative units. This calibrated formulation of N_2O emissions was found to explain over 84% of the variance of field observations (Zhou et al., 2015), yet the model was only constrained by 732 field observations of N_2O emissions. We updated the model by fitting the N_2O emissions to new observations extended to 2,740 flux observations across 345 sites in the world (see Text S1, Tables S1~S2). The extended dataset covers a wider range of environmental conditions and agricultural management practices compared to our previous work and other similar studies (Gerber et al., 2016; Shcherbak et al., 2014) (Tables S3). The N_2O emissions (E) of the updated SRNM model is described as:

$$E_{ijt} = \alpha_{ij} R_{ijt}^2 + \beta_{ij} R_{ijt} + \gamma_{ij} + \varepsilon_{ijt} , \quad (1a)$$

where

$$\alpha_{ij} \sim N\left(X_k^T \lambda_{ijk}, \sigma_{ijk}^2\right),\ \beta_{ij} \sim N\left(X_k^T \phi_{ijk}, \sigma_{ijk}'^2\right),\ \gamma_{ij} \sim N\left(X_k^T \varphi_{ijk}, \sigma_{ijk}''^2\right), \quad (1b)$$

$$\lambda_{ijk} \sim N\left(\mu_{ijk}, \omega_{ijk}^2\right),\ \phi_{ijk} \sim N\left(\mu_{ijk}', \omega_{ijk}'^2\right),\ \varphi_{ijk} \sim N\left(\mu_{ijk}'', \omega_{ijk}''^2\right),\ \varepsilon_{ijt} \sim N\left(0, \tau^2\right), \quad (1c)$$

and i denotes the sub-function of N_2O emissions (i=1, 2, …, I). j represents the type of crop (j=1-9, i.e., represents maize, wheat, paddy rice, vegetables, fruits, potatoes, oil crops, legume, and the other crops). k is the index of climate factors or soil property (k=1-6, i.e., soil organic carbon content, clay content, bulk density, soil pH, air temperature and the sum of precipitation and irrigation). E_{ijt} denotes the N_2O emission rate (kg N ha^{-1} yr^{-1}) predicted for crop type j in year t in the ith type of regions. R_{ijt} is N application rate (kg N ha^{-1} yr^{-1}). α, β, and γ are described as linear functions of climate or soil factors X_k (Table S2). γ is an intercept denoting the background emission, $\alpha R^2+\beta R$ represents the fertilizer-induced emission, $\alpha R+\beta$ being the emission factor, and ε is the residual term. The random terms λ, ϕ, φ, and ε are assumed to be independent and normally distributed. μ is the mean applied N effect for α and β or the mean emission baseline for γ. σ, ω, and τ are standard deviations. All the parameter mean values and standard deviations in each of sub-functions were estimated by the Bayesian Recursive Regression Tree version 2 (BRRT v2) (Zhou et al., 2015), constrained by the extended dataset. The estimated parameter values are presented in Table S4. The detailed methodology of the BRRT v2 algorithm and the associated procedures can be found in Zhou et al. (2015).

2.2 New model inputs of N-fertilizers and irrigation

The updated SRNM model is forced by multiple gridded input datasets, including new datasets describing N inputs and irrigation to croplands. For N inputs, we first collected nationwide surveys of county-scale (the third-level administrative division) synthetic N fertilizer applied to croplands (F_{SN}, kg N yr^{-1}) for ~ 2900 counties in Mainland China, Taiwan, Hong Kong, and Macau for the period 1990-2014. These data were further disaggregated by nine types of crop,

based on the crop-specific, provincial data of R_{ijt} from the Statistics of Cost and Income of Chinese Farm Produce (http://tongji.cnki.net/overseas). In addition, China has experienced changes of County-scale administrative divisions, such as aggregation, disaggregation, and name changes, so we harmonized the temporal evolution of F_{SN} to fit the latest administrative divisions (http://geodata.pku.edu.cn), based on the historical trajectories summarized by the Ministry of Civil Affairs of China (http://xzqh.mca.gov.cn/). More details can be found in Text S2. Second, we estimated annual N in livestock manure, human excreta, and crop residues returned to croplands by the *Eubolism* model at county scale (Chen, Chen, & Sun, 2010), based on county-scale activity data, such as the numbers of livestock by animal, rural population, and yields by crop type. The *Eubolism* model has been evaluated against multi-site observations in highly-fertilized cropping areas across China (see Text S3). Third, dry and wet deposition of N species were quantified by the global aerosol chemistry climate model LMDZ-OR-INCA at a horizontal resolution of 1.27° latitude by 2.5° longitude (Wang et al., 2017), in which wet N deposition fluxes have been validated by a recent global dataset (Vet et al., 2014). Finally, crop-specific N application rates (R_{ijt}) were calculated as county-scale N input totals (i.e., synthetic fertilizers, manure, human excreta, crop residues, and N depositions) divided by the associated sowing areas that were obtained from the statistical yearbooks of 31 provinces (http://tongji.cnki.net/overseas). This new county-scale dataset of R_{ijt} was then resampled into a 1-km grid map based on the dynamic cropland distributions (Liu et al., 2014). We assumed a maximum N fertilizer application rate of 700 kg N ha^{-1} based on a previous study (Carlson et al., 2017).

The second new gridded dataset is cropland irrigation application rate for the period 1990-2014. We first collected prefectural-level (i.e., the second-level administrative division) cropland irrigation amounts from two nationally-coordinated surveys: the 2nd National Water Resources

Assessment Program for the period 1990-2000 (China Renewable Energy Engineering Insitute, 2014) and the Water Resources Bulletins of 31 provinces for the rest of period 2001-2014 (www.mwr.gov.cn/english/publs/). Both surveys had an identical methodology, including definitions, survey units, field surveys or measurements, and quality assurance. The detailed survey methodology is described in Text S4. It should be noted that cropland irrigation used here did not include water applied for aquaculture that accounts for less than 5% of agricultural irrigation (Zhu, Li, Li, Pan, & Shi, 2013). Cropland irrigation rates (mm yr^{-1}) at the prefectural level were then calculated as cropland irrigation amounts divided by sowing areas. Similarly with R_{ijt}, these prefectural-scale cropland irrigation application rates were then disaggregated by resampling to 1-km gridded cropland maps for the period 1990-2014, and such rates were simply assumed same for each crop. Other data sources for model inputs can be found in Text S5, including soil properties and climate factors relevant to N_2O emissions.

2.3 Model validation and comparison

Process-based models were run using the same input data, and their outputs were compared with the results of the updated SRNM model. These process-based models include the Dynamic Land Ecosystem Model (DLEM) (Tian et al., 2015), the Organising Carbon and Hydrology In Dynamic Ecosystems (ORCHIDEE-OCN) (Zaehle & Friend, 2010), the Daily Century Model (DAYCENT) (Del Grosso et al., 2009), and Vegetation-Integrated Simulator for Trace Gases (VISIT) (Ito & Inatomi, 2012). Nitrification and denitrification processes in these models are expressed as functions of available substrates (NH+ 4or NO− 3 concentration), reaction rates, soil temperature and water content, but with different formulations and parameterizations (Tian et al., 2018). The results from atmospheric inversion of Saikawa et al. (2014), constrained by global measurements of N_2O atmospheric concentrations, were also compared with the estimated N_2O emissions. The new inversion was also conducted by replacing emissions from

this study for *a priori* agricultural soil emissions for China in the Bayesian inversion model (Saikawa et al., 2014). The detailed methodology and parameter calibration of the process-based models and the inversion model can be found in previous studies (Saikawa et al., 2014; Tian et al., 2018). In addition, the national estimates of cropland N_2O emissions were compared with the state-of-the-art emission inventories, including the Food and Agriculture Organization Emission Database (FAOSTAT) (FAO, 2018), the Emissions Database for Global Atmospheric Research (EDGAR version 4.3.2) (Janssens-Maenhout et al., 2019), and the Greenhouse Gas and Air Pollution Interactions and Synergies (GAINS) (Winiwarter, Höglund-Isaksson, Klimont, Schöpp, & Amann, 2018), U.S. Environmental Protection Agency (USEPA) report (USEPA, 2012), and three China's National Communication Reports (CNCR; National Development and Reform Commission, 2017) submitted to the UNFCCC for years 1994, 2005, and 2012. Note that EDGAR, FAOSTAT and GAINS estimates were derived using the methodology of the 2006 IPCC Guidelines for National Greenhouse Gas Inventories (IPCC, 2006) and national fertilizer data from the FAO.

2.4 Attribution of N_2O emission trends

We applied the Logarithmic Mean Divisia Index (LMDI) (Ang, 2015; Guan et al., 2018) to attribute N_2O emission trends to different driving factors. The LMDI was chosen because of its path independence, consistency in aggregation, and ability to handle zero values (Ang, 2015). The LMDI analysis compares a set of driving factors between the base and final year of a given period, and explores the effects of these factors on the change in China's cropland-N_2O emissions over that period. The detailed methodology of LMDI can be found in Ang (2015). According to previous modeling studies (Guan et al., 2018), we decomposed cropland-N_2O emissions into a combination of different drivers: total sowing area (A_k, ha), the share of nine different crops to total sowing area (m_{jk}, %) also known as crop mix, N application rate (R_{jk}, kg

N ha^{-1} yr^{-1}), and the emission intensity (e_{jk}, %) per crop type and region:

$$E_k = \sum_j \left(A_k \times \frac{A_{jk}}{A_k} \times \frac{N_{jk}}{A_{jk}} \times \frac{E_{jk}}{N_{jk}} \right) = \sum_j \left(A_k \times m_{jk} \times R_{jk} \times e_{jk} \right), \quad (2)$$

where region k=1-8 corresponds to China, the Northwest, the Northeast Plain, the North China Plain, the lower reach of Yangtze River basin, the Southwest, the Northwest, and Qinghai-Tibet Plateau; A_{jk} is the sowing area of crop j in cropping region k; N_{jk} and E_{jk} are N-fertilizer application amount and croplands N_2O emission of crop j in cropping region k, respectively. It should be noted that e_{jk} is defined as cropland-N_2O emission per unit of N_{jk}, which is different from the emission factor defined in the 2006 IPCC Guidelines, and represents the gross emission intensity at a given N application level. The change of E of region k in the year t compared to the year $t-1$ is computed as

$$\begin{aligned} \Delta E_k &= \sum_j w_{jk} \ln\left(\frac{A_k^t}{A_k^{t-1}} \right) + \sum_j w_{jk} \ln\left(\frac{a_{jk}^t}{a_{jk}^{t-1}} \right) + \sum_j w_{jk} \ln\left(\frac{R_{jk}^t}{R_{jk}^{t-1}} \right) + \sum_j w_{jk} \ln\left(\frac{e_{jk}^t}{e_{jk}^{t-1}} \right). \\ &= \Delta E_A + \Delta E_m + \Delta E_R + \Delta E_e \end{aligned} \quad (3)$$

Here, $w_{jk} = \left(E_{jk}^t - E_{jk}^{t-1} \right) / \left(\ln E_{jk}^t - \ln E_{jk}^{t-1} \right)$ is a weighting factor called the logarithmic mean weight (Ang, 2015). ΔE_A, ΔE_m, ΔE_R, and ΔE_e, are changes in E, corresponding to change in total sowing area, shift in crop mix, change in N application rate, and emission intensity, respectively. The change of ΔE between base and final years is then calculated by the cumulative ΔE between adjacent years. The sign of the ΔE indicates a positive or negative effect of the factor on the change of cropland N_2O emissions between the base and final years, and the potential impacts of nationwide policy interventions related to fertilizer application, crop type and sowing area.

3. Results

3.1 Model performance

Combining the new N inputs and irrigation data and the other forcing datasets with the updated SRNM model, we estimated a mean annual N_2O emission from China's croplands of 0.62 ± 0.06 Tg N yr^{-1} during the period 1990-2014 (one standard deviation due to inter-annual variability of N_2O emissions), with the spatial distribution shown in Fig. 1a. The validity of our N_2O emission estimates was supported by internal cross-validation at 345 sites (R^2=0.88 and 0.90 for upland crops and paddy rice, respectively, Fig. 1b). In addition, our SRNM model outputs performed well in reproducing the spatial contrast and long-term inter-annual variability of N_2O emissions as well as the sensitivity of N_2O emission to environmental changes (Figs S1 and S2). In addition, the N_2O emissions were corroborated against independent simulations from four process-based models and the estimates from the atmospheric inversion (R^2 = 0.91 and 0.66, respectively, Fig. 1c). This new estimate of China's cropland N_2O emissions is consistent with the USEPA report (0.59 Tg N yr^{-1}) (USEPA, 2012), and in general fell with the range of process-based models (0.35 to 0.73 Tg N yr^{-1}, Fig. 1c). However, it exceeded emission estimates provided by EDGAR v4.3.2 product (Janssens-Maenhout et al., 2017) by 43%, the FAOSTAT by +55%, the GAINS by 67%, and the CNCR for years 1994 and 2005 by 36% (*t*-test at the 95% level, Fig. 1d), but was comparable to the latest CNCR report for the year 2012 (0.78 Tg N yr^{-1}).

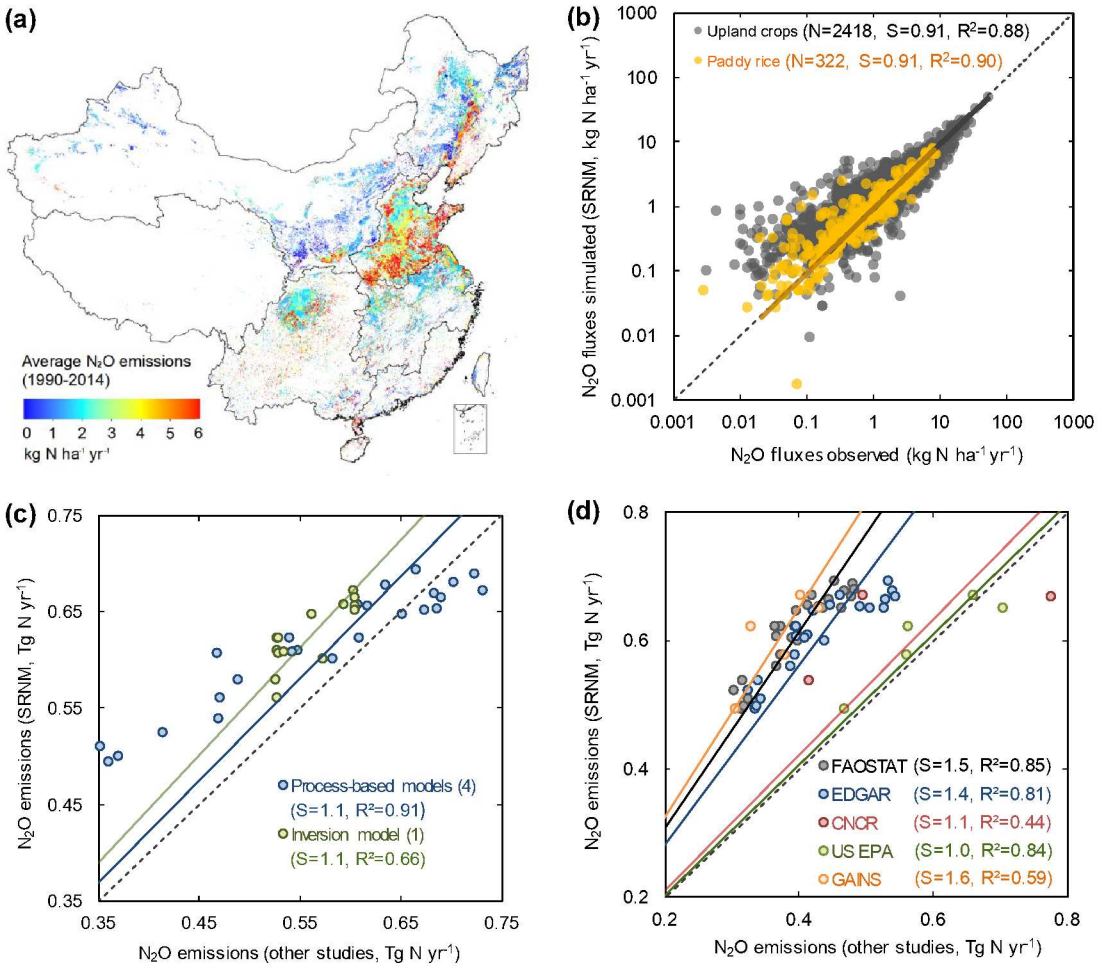

Figure 1. Validation of China's cropland N_2O emissions from the updated SRNM model. (a) Pattern of mean annual N_2O emissions simulated (1990-2014). (b) Model performance of the simulated cropland N_2O fluxes. (c) Comparison of annual cropland N_2O emissions against the means of process-based models (1990-2014) and inversion models (1996-2008). Each point represents the estimated N_2O emissions from Chinese croplands for a certain year. Numbers in brackets show the number of models. (d) Comparison of annual cropland N_2O emissions with the emission inventories, including FAOSTAT (1990-2014), EDGAR v4.3.2 (1990-2012), CNCR (1994, 2005, 2012); USEPA (1990-2005), and GAINS (1990, 1995, 2000, 2005, 2010). Note that N, S, and R^2 denote the number of measurements, slope of regression line, and coefficient of determination, respectively.

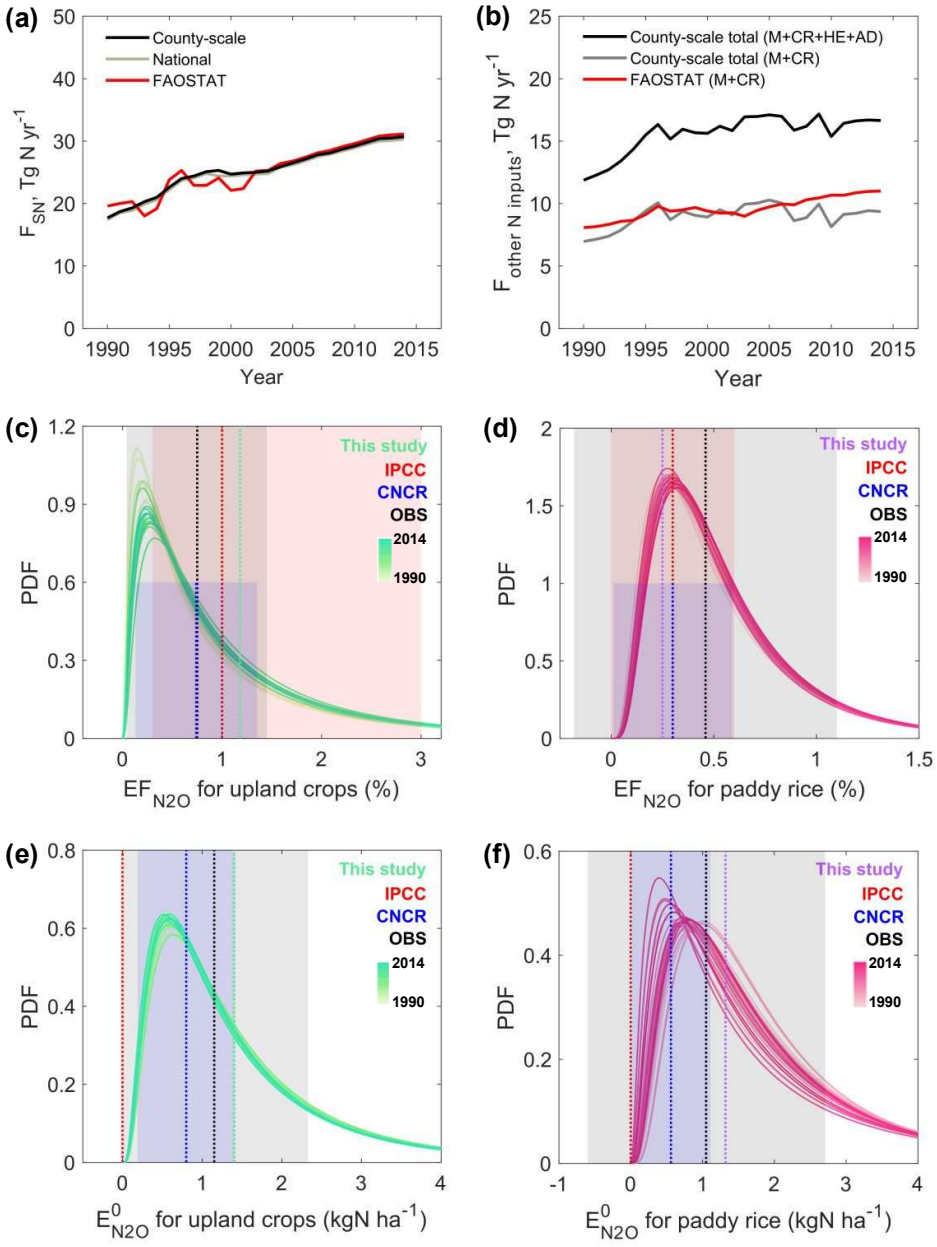

Figure 2. Comparisons of N inputs, emission factor and 'background' anthropogenic emissions of cropland N_2O in China. (**a**) Synthetic fertilizers applied to croplands. (**b**) Other N inputs, including manure (M), crop residues (CR), human excreta (HE) returned to croplands, and atmospheric deposition (AD) over croplands. (**c**) Lognormal probability density function of emission factor for all upland crops based on gridded results during the period 1990-2014, where the dashed lines indicate the median values, and shaded areas represent standard deviation for this study and observed values (OBS) or 95% confidence interval for the IPCC and the CNCR. (**d**) Same as panel **c** but for paddy rice. (**e**) Same as panel **c** but for background emission (E^0) of upland rice. (**d**) Same as panel **c** but for E^0 of paddy rice. Note that the definition of FAOSTAT, IPCC, CNCR, and OBS can be found in the text.

The differences between our estimates and other inventories were primarily attributed to the updates of N input data, emission factors, and 'background' anthropogenic emissions from soil residual N (Fig. 2). First, our county-scale estimation of synthetic N fertilizer application was almost identical to the national statistics and FAOSTAT data (Fig. 2a), whereas the other N inputs were substantially larger because the inclusion of human excretion and atmospheric deposition over croplands (Figs 2b and S3). Second, our estimate of the nationally-averaged N_2O emission factor (EF) for upland crops was larger than IPCC Tier 1 default by 20% (Fig. 2c), but the EF was −17% lower for paddy rice (Fig. 2d and Text S6). Furthermore, the 'background' anthropogenic emissions of N_2O (γ) due to the legacy effect resulting from historical soil N accumulation were estimated to be 1.40±0.04 kg N ha^{-1} yr^{-1} for upland crops and 1.30±0.05 kg N ha^{-1} yr^{-1} for paddy rice in this study (Figs 2e and 2f), while they were not fully accounted for by the IPCC Tier 1 inventories. Our estimates of this term were larger than the values used in the CNCR (0.80 and 0.56 kg N ha^{-1} yr^{-1}), but generally agreed with the *in situ* observations (OBS) with zero N input (1.2 ± 1.2 and 1.0 ± 1.7 kg N ha^{-1} yr^{-1} based on 168 and 54 sites, respectively).

3.2 Trend in cropland N_2O emissions in China

Over the period 1990-2014, cropland N_2O emissions showed a persistent and widespread increase (Fig. S4), because of the significant increase in N inputs to croplands. However, the rate of this increase slowed down from 11.2 Gg N yr^{-2} ($P < 0.001$) before 2003 to 2.8 Gg N yr^{-2} ($P = 0.02$) afterwards (Figs 3a and 3b), a turning point detected by Pettitt's test (Pettitt, 1979) ($P < 0.001$). This slower, insignificant growth of cropland-N_2O emissions was confirmed by the process-based models with the same forcing datasets (19.8 Gg N yr^{-2} for 1990-2003, $P < 0.001$; 4.8 Gg N yr^{-2} for 2003-2014, $P = 0.15$; Fig. 3b). We then divided the past 25 years into two periods covering 1990-2003 (P1) and 2003-2014 (P2). Regionally,

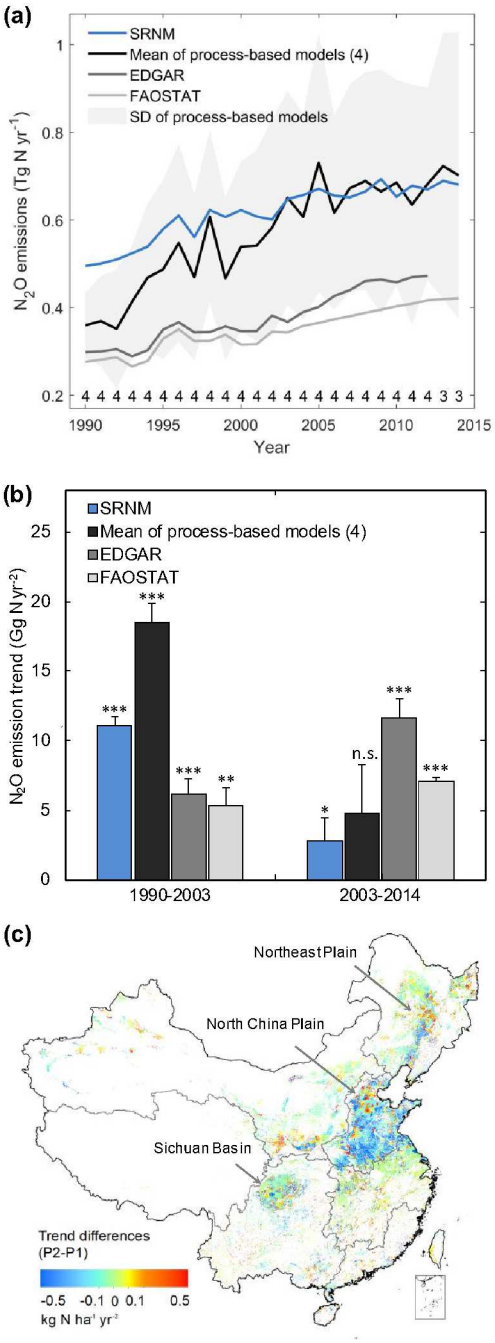

Figure 3. The inter-annual variability of cropland-N_2O emissions in China. (a) Temporal evolution of annual cropland-N_2O emissions based on the updated SRNM model, an ensemble of four process-based models, and previous inventories (EDGAR v4.3.2 and FAOSTAT). Shaded area indicates the standard deviation of the results from process-based models. Numbers at the bottom show the number of process-based models available for each year. (b) Trends in cropland-N_2O emissions based on different approaches for two different periods (P1: 1990-2003, P2: 2003-2014); ***, **, and * indicate significance of the trends at the 99.9%, 99% and 95% confidence interval, respectively; n.s., not significant. (c) Pattern of the difference in N_2O trends between the two periods.

approximately 64% of the Chinese sowing area experienced a weakened growth or even a decline of N_2O emissions in P2, primarily located in major cropping areas such as the North China Plain, the Sichuan Basin, and a part of the Northeast Plain (Fig. 3c), while the rest showed a growth in emissions, mainly in Heilongjiang province and the Northwest China (Fig. 3c). By contrast, the estimates provided by EDGAR v4.3.2 have suggested enhanced growth of cropland-N_2O emissions across China (Figs 3b and S5). The estimated growth rate of cropland-N_2O emissions in EDGAR v4.3.2 after 2003 (11.6 Gg N yr^{-2}, $P < 0.001$) is much larger than that for 1990-2003 (6.2 Gg N yr^{-2}, $P < 0.001$; Fig. 3b). Differences in emission trends between our estimates and the EDGAR product are mainly focused around the North China Plain (Fig. S5).

3.3 Drivers of China's cropland-N_2O emission trends

The decomposition analysis in Fig. 4 shows the contribution of each of the four drivers to the change in cropland-N_2O emissions in China and its seven major cropping regions. For P1, the trend of emissions was associated with a growth of N_{rate} for all crops (Fig. 4a), mainly located in the North China Plain and the Northeast Plain (Figs 4c-4d). For P2, the slower growth in cropland-N_2O emissions across China was driven by the downward influences from the reduced N_{rate} and emission intensities, which largely offset the strong expansion of sowing areas particularly in the Northeast Plain (Figs 4a and 4c). By contrast, the shifts in the crop mix and in emission intensity contributed marginally to changes in emissions in both periods (Fig. 4a).

Contributions of the four driving factors to cropland-N_2O emission trends differed between cropping regions (Figs 4b-4h). During the period P1, the trend in cropland-N_2O emissions was explained by the growth of N_{rate} in most of the major cropping regions, except for the Northwest

where there was deceased emission intensity. During the period P2, sowing area expansion became the largest contributor to the positive cropland-N_2O emission trends in the Northeast Plain, the Northwest, the Southwest, as well as the lower reaches of the Yangtze River basin. However, the decrease in emission intensity dominated the change in cropland-N_2O emissions in the North China Plain, and N_{rate} contributed to the changes in the Southeast and Qinghai-Tibet Plateau.

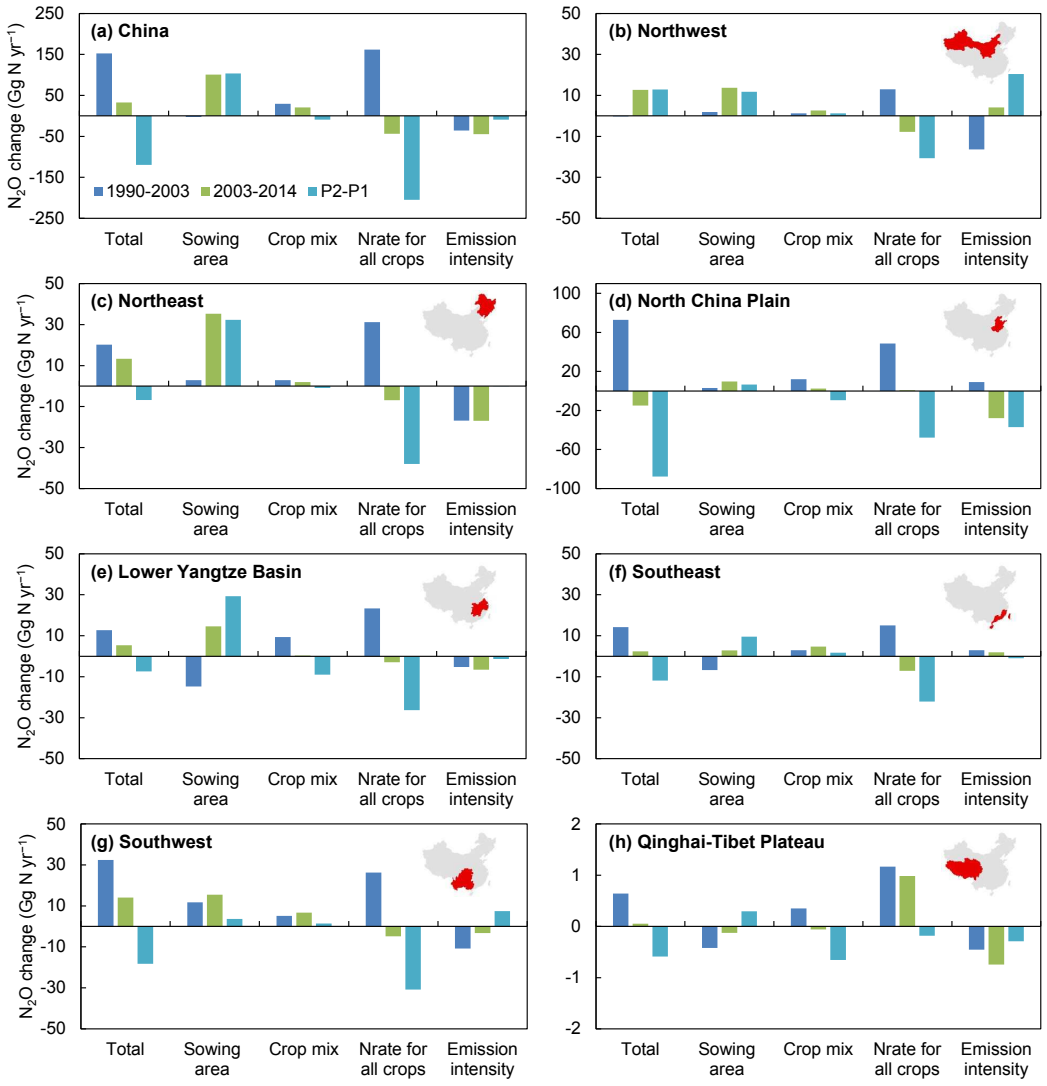

Figure 4. Contribution of different drivers to the change in cropland-N_2O emissions by cropping region during 1990-2003 (P1) and 2003-2014 (P2). a. China; **b**. northwest China; **c**. northeast China; **d**. North China Plain; **e**. lower Yangtze Basin; **f**. southeast China; **g**. southwest China; **h**. Qinghai-Tibet Plateau. Note varying vertical-axes. The length of each bar reflects the contribution of each factor during the corresponding period.

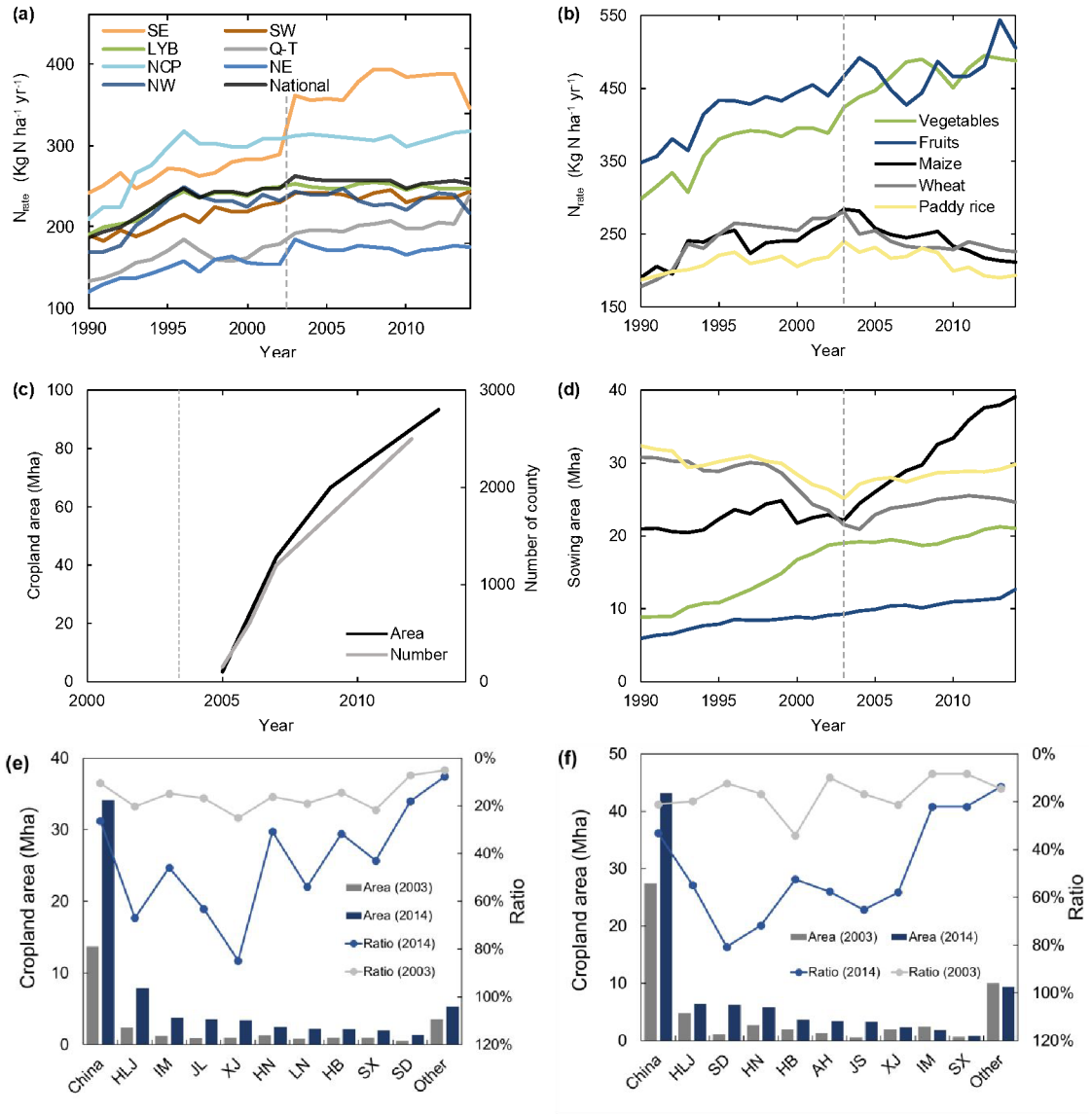

Figure 5. Temporal evolution of agricultural management in China. a. N_{rate} in 7 major cropping regions. **b.** N_{rate} by crops. **c.** National sowing areas and county number applied by the Nationwide Soil Testing and Formulation Fertilization Program. **d.** National sowing areas by crops. **e.** Provincial areas and ratio of croplands using mechanically-aided deep placement of fertilizers in 2003 and 2014, where the ratio is calculated as the croplands using this technology divided by national cropland area. **f.** Same as panel **e** but for crop residues returned to croplands. The seven cropping regions include Southeast (SE), Southwest (SW), Lower Yangtze Basin (LYB), Qinghai-Tibet Plateau (Q-T), North China Plain (NCP), Northeast (NE) and Northwest (NW). HLJ: Heilongjiang, IM: Inner Mongolia, JL: Jilin, XJ: Xinjiang, HN: Henan, LN: Liaoning, HB: Hebei, SX: Shanxi, SD: Shandong, AH: Anhui, JS: Jiangsu

Overall, in period P2 (after 2003), the reduction of N_{rate} dominated the slowdown of cropland-N_2O emissions in China. According to nationwide statistics, China's N_{rate} showed a clear

reversal in trend around 2003, from an increasing rate of +5.1 kg N ha^{-1} yr^{-2} in P1 to a decrease of –0.7 kg N ha^{-1} yr^{-2} in P2, although it varied across different cropping regions (Fig. 5a). Similar decreases in crop-specific N_{rate} were found for wheat, maize, and paddy rice, but not for vegetables and fruits, all with Pettitt's test (Fig. 5b, $p < 0.001$). Interestingly, these change points were, in general, coincident with changes in cropland-N_2O emissions in China. The reductions of N_{rate} were mainly due to declines in synthetic fertilizer uses, particularly in the eastern and central China, the Yunnan-Guizhou Plateau, and the North China Plain (Fig. S6).

4. Discussion

Reliable estimation of cropland-N_2O emissions and their drivers is fundamental to the development of policy for sustainable N management. Previous estimates have shown large differences in the magnitude and temporal evolution of annual cropland-N_2O emissions. This has mainly been due to the lack of high-resolution data on agricultural management and of spatial representation in the models. Our updated SRNM model, along with new, crop-specific gridded datasets of N inputs and irrigation, permits a new insight into the spatial contrast and inter-annual variability of cropland-N_2O emissions, and associates these with policy-driven technological adoption and environmental changes.

The reduced N_{rate} suggests that national N use efficiency of fertilizers has improved over recent decades, given that there was no reduction in per-area crop yields according to the national statistics (Sun & Huang, 2012). One of the most effective methods of making fertilizer use more efficient is to match the supply of nutrients with demand during field application (Richards et al., 2015). Such an approach was one of targets of the Nationwide Soil Testing and Formulation Fertilization Program, launched in the early 2000s (Table S7). This program started with staple crops, which account for ~50% of national N inputs on average, but after

2010 it extended to a number of cash crops. These improved N use efficiencies for staple crops were also found in the most recent study (Zou et al., 2018). According to national statistics (Sun & Huang, 2012), such technologies increased in prevalence on croplands from 3.3 million ha in 200 counties, to ~93 million ha in 2,498 counties (Fig. 5c). In addition, spatial re-allocation of crops has extensively happened in China over recent decades, and is characterized by an emerging shift from peri-urban areas in the South and Central China (high N rate) to rural areas in the North (low N rate) because of urbanization (Fig. S7; Zou et al., 2018). Although the effectiveness of the Nationwide Soil Testing and Formulation Fertilization Program on the N_{rate} is difficult to quantify at the regional scale, these measures contributed to the decline in N_{rate} across China (Chen et al., 2014).

The increased sowing area was identified as the second important driver of cropland-N_2O emission trends in P2 that partially offset the effect of decreasing N_{rate}. The shift in crop mix resulted in positive emission trends in P1, but made negligible contributions across most cropping regions in P2. Specifically, sowing areas by crop have changed in line with multiple nationwide crop structural transition programs in China. During the period 1990-2003, the Government of China encouraged the growth of cash crops to meet increased consumption requirements. According to national statistics, the sowing areas of vegetables and fruits increased by 115% and 57% in the P1 (Fig. 5d), respectively. Meanwhile, the areas sown to wheat and paddy rice declined by –30% and –22%, and sowing area of maize remained at the level as that in 1990. This structural transition in cropping patterns that occurred in P1 resulted in more cropland-N_2O emissions, because vegetables and fruits, which constitute the major area of cash crops, have an emission factor two times higher than that of staple crops (Dobbie & Smith, 2003). During P2 (after 2003), the Government of China aimed to stabilize the production of cash crops, but to also restore the production of cereal crops. As a result, the

458 sowing areas of staple crops increased by 36%, while the sowing areas of vegetables, fruits,
459 and oil crops were increased by only 11% (Fig. 5d). Compared to the period P1, this shift in
460 crop mix in P2 exerted a lower upward pressure on cropland-N_2O emissions, particularly in the
461 major cropping regions. The results underscore the significance of land-use changes to the
462 spatial and inter-annual variabilities of N_2O emissions.
463
464 Our results show that emission intensity decreased during both periods and had a negative
465 effect on the growth of cropland-N_2O emissions across most of the cropping regions. Scenario
466 simulations based on the SRNM (see Text S7) suggest that N_{rate} was the dominant factor
467 controlling the emission intensity trend, followed by soil organic carbon (SOC) and water
468 inputs (Fig. S8). Increased SOC offset 19% and 51% of the negative effects from N_{rate} for P1
469 and P2, respectively. Thus whilst C sequestration can help offset some of the cropland
470 emissions of CO_2, a recent study suggests that carbon emission equivalents of non-CO_2 GHG
471 emissions are currently ~12 times greater than carbon uptake by Chinese croplands over 100-
472 year time horizon (B. Gao et al., 2018). SOC also played a role in increasing N_2O emissions
473 with a positive correlation between N_2O emissions and SOC reported in field (Figueiredo,
474 Enrich‐Prast, & Rütting, 2016), laboratory studies (Jäger, Stange, Ludwig, & Flessa, 2011),
475 meta-analyses (Bouwman, Boumans, & Batjes, 2002; Charles et al., 2017), and data mining
476 analysis (Perlman et al., 2014). The postive effect of SOC could be explained by high SOC
477 providing sources of energy, C and N for nitrifying and denitrifying microorganisms, and
478 creating anaerobic conditions favoring the oxidation-reduction reaction for denitrification
479 (Charles et al., 2017).
480
481 At present, the attribution of trends in cropland-N_2O emissions to driving factors contains some
482 uncertainties. Other potential factors responsible for the decline in emissions seem also to be

483 important, but were difficult to consider explicitly. These include, among others, changes in
484 crop cultivars (Zhang, Fan, Wang, & Shen, 2009), cultivation technology improvements places
485 (Jiang et al., 2018), timing (Jiang et al., 2018; Wang et al., 2016) and placement methods (Chen,
486 Wang, Liu, Lu, & Zhou, 2016), and changes in fertilizer type (Bouwman et al., 2002). For
487 example, multiple field trials for staple crops in China suggest a significant increase in N-use
488 efficiency (ratio of yield to N_{rate}) associated with cultivar improvement over recent decades (de
489 Dorlodot et al., 2007). However, this does not mean a coincident reduction of N_{rate} because
490 crop yields (i.e., per-area crop production of these new cultivars) grew synergistically, and thus
491 might require more fertilizer per unit of cropped area. The improvement of cultivation
492 technology plays an important role in influencing cropland-N_2O emissions. For example, the
493 proportion of croplands using mechanically-aided deep placement of fertilizers increased from
494 11% in 2003 to 26% at present, particularly in the north of China (Fig. 5e), decreasing the N
495 losses and thereby cropland-N_2O emissions. Increasing the return of crop residues, also
496 particularly in the North China Plain, has been hypothesized as an emerging driver for the
497 change of N_{rate}. In these regions, crop residues returned to croplands accounted for from 21%
498 in 2003 to 33% of croplands in 2014 (Fig. 5f), increasing the potential to replace the application
499 of synthetic fertilizers, and to change carbon and N biogeochemical cycles in soils (Chen, Li,
500 Hu, & Shi, 2013; Xia et al., 2018). However, the effect of crop residues on cropland-N_2O
501 emissions is more complex and modified by the prevalence of aerobic and anaerobic soil
502 conditions (Xia et al., 2018), and also the chemical composition of the plant material (S. Gao
503 et al., 2018).
504
505 In summary, the results from this study underline the advantage of high-resolution agricultural
506 activity data and emission intensity detailed by crop type, land-use dynamics and technology
507 improvement to understand the change in cropland-N_2O emissions. Most of the state-of-the-art

emission inventories that aim to quantify global N_2O emissions, fail to capture either the magnitude or temporal trends in China. This is because firstly, an IPCC default EF of 1% assumes a constant relationship between N input and N_2O emissions. This cannot reproduce the spatial and temporal responses of N_2O emission to environmental changes. Secondly, emission inventories, in general, disaggregate national-scale or low-resolution fertilizer and irrigation data into gridded maps to generate cropland-N_2O emission patterns. This would be likely to lower emission estimates from regions predominantly fertilized at high N inputs (e.g., the North China Plain), while increasing emission estimates from under-fertilized areas (e.g., the Northeast Plain). Process-based terrestrial biosphere models (TBM) still face many challenges in modelling changes in cropland-N_2O emissions (Sandor et al. 2018). Though most of them consider the biotic and abiotic processes involved N_2O production, they also generate divergent estimates of cropland-N_2O emissions and spatio-temporal patterns (Tian et al., 2018). Possible reasons for divergent estimates among TBMs are the incomplete model representation of N_2O emissions in response to agricultural management practices and uniform response functions of the N_2O flux to environmental conditions (e.g., SOC). Improving the representation of crop-specific agricultural activity data and the regional adoptions of N_2O flux response are recommended for future projections.

The updated SRNM model for China's cropland-N_2O emissions could be extended to other countries for updating their cumulative emissions and their contributions to global historical radiative forcing and ozone depletion. The decomposition of cropland-N_2O emission trends to underlying drivers could facilitate the tracking of key indicators that require significant change. Our modeling results also highlight that technological adoption was intertwined with policy interventions in China. We argue that designing more realistic future scenarios for technological adoption will increase the likelihood that policies will be implemented to set

targets and incentives for cropland-N_2O emission mitigation.

ACKNOWLEDGMENT

This study was supported by the National Natural Science Foundation of China (41671464; 7181101181), the National Key Research and Development Program of China (2016YFD0800501; 2018YFC0213304), 111 Project (B14001), the GCP-INI Global N_2O Budget and the INMS Asia Demo Activities. The input of P.S. contributes to the UK-China Virtual Joint Centre on Nitrogen "N-Circle" funded by the Newton Fund *via* UK BBSRC/NERC (BB/N013484/1). We acknowledged Eric Ceschia, Kristiina Regina, Dario Papale, and the NANORP for sharing a part of observation data.

REFERENCES

Alexandratos, N., & Bruinsma, J. (2012). *World agriculture towards 2015/2030: The 2012 Revision*. *ESA Working Paper* (Vol. 12, No. 3). FAO, Roma. https://doi.org/10.1016/S0264-8377(03)00047-4

Allen, M. R., Coninck, H. D., Connors, S., Engelbrecht, F., Ferrat, M., Ford, J., … Taylor, M. IPCC Special Report on Global Warming of 1.5°C. In Press.

Ang, B. W. (2015). LMDI decomposition approach: A guide for implementation. *Energy Policy*, *86*, 233–238. https://doi.org/10.1016/j.enpol.2015.07.007

Bouwman, A. F., Boumans, L. J. M., & Batjes, N. H. (2002). Emissions of N_2O and NO from fertilized fields: Summary of available measurement data. *Global Biogeochemical Cycles*, *16*(4), 6-1-6–13. https://doi.org/10.1029/2001GB001811

Carlson, K. M., Gerber, J. S., Mueller, N. D., Herrero, M., MacDonald, G. K., Brauman, K. A., … West, P. C. (2017). Greenhouse gas emissions intensity of global croplands. *Nature*

Climate Change, *7*(1), 63–68. https://doi.org/10.1038/nclimate3158

Charles, A., Rochette, P., Whalen, J. K., Angers, D. A., Chantigny, M. H., & Bertrand, N. (2017). Global nitrous oxide emission factors from agricultural soils after addition of organic amendments: A meta-analysis. *Agriculture, Ecosystems and Environment*, *236*, 88–98. https://doi.org/10.1016/j.agee.2016.11.021

Chen, H., Li, X., Hu, F., & Shi, W. (2013). Soil nitrous oxide emissions following crop residue addition: A meta-analysis. *Global Change Biology*, *19*(10), 2956–2964. https://doi.org/10.1111/gcb.12274

Chen, M., Chen, J., & Sun, F. (2010). Estimating nutrient releases from agriculture in China: An extended substance flow analysis framework and a modeling tool. *Science of the Total Environment*, *408*(21), 5123–5136. https://doi.org/10.1016/j.scitotenv.2010.07.030

Chen, X., Cui, Z., Fan, M., Vitousek, P., Zhao, M., Ma, W., … Zhang, F. (2014). Producing more grain with lower environmental costs. *Nature*, *514*(7523), 486–489. https://doi.org/10.1038/nature13609

Chen, Z., Wang, H., Liu, X., Lu, D., & Zhou, J. (2016). The fates of ^{15}N-labeled fertilizer in a wheat–soil system as influenced by fertilization practice in a loamy soil. *Scientific Reports*, *6*, 34754. Retrieved from https://doi.org/10.1038/srep34754

China Renewable Energy Engineering Insitute. (2014). *Evaluation of China's water resources and its exploitation and utilization*. Beijing: China Water & Power Press.

National Development and Reform Commission (NDRC) (2017). *The People's Republic of China first biennial update report on climate change*. Retrieved from http://qhs.ndrc.gov.cn/dtjj/201701/W020170123346264208002.pdf

de Dorlodot, S., Forster, B., Pagès, L., Price, A., Tuberosa, R., & Draye, X. (2007). Root system architecture: opportunities and constraints for genetic improvement of crops. *Trends in Plant Science*, *12*(10), 474–481. https://doi.org/10.1016/j.tplants.2007.08.012

582 Del Grosso, S. J., Ojima, D. S., Parton, W. J., Stehfest, E., Heistemann, M., DeAngelo, B., &
583 Rose, S. (2009). Global scale DAYCENT model analysis of greenhouse gas emissions
584 and mitigation strategies for cropped soils. *Global and Planetary Change*, *67*, 44–50.
585 https://doi.org/10.1016/j.gloplacha.2008.12.006
586 Dobbie, K. E. , & Smith, K. A. (2003). Nitrous oxide emission factors for agricultural soils in
587 Great Britain: the impact of soil water-filled pore space and other controlling variables.
588 *Global Change Biology*, *9*(2), 204-218. https://doi.org/10.1046/j.1365-2486. 2003.00563.x
589 Ehrhardt, F., Soussana, J. F., Bellocchi, G., Grace, P., McAuliffe, R., Recous, S., ... & Basso,
590 B. (2018). Assessing uncertainties in crop and pasture ensemble model simulations of
591 productivity and N_2O emissions. *Global Change Biology*, *24*(2), 603-616.
592 https://doi.org/10.1111/gcb.13965
593 Figueiredo, V., Enrich‐Prast, A., & Rütting, T. (2016). Soil organic matter content controls
594 gross nitrogen dynamics and N_2O production in riparian and upland boreal soil. *European*
595 *Journal of Soil Science*, *67*(6), 782–791. https://doi.org/10.1111/ejss.12384
596 Flörke, M., Schneider, C., & McDonald, R. I. (2018). Water competition between cities and
597 agriculture driven by climate change and urban growth. *Nature Sustainability*, *1*, 51–58.
598 https://doi.org/10.1038/s41893-017-0006-8
599 Food and Agricultural Organization of the United nations (FAO). FAOSTAT data. Retrieved
600 June 18, 2018, from http://www.fao.org/faostat/en/#data
601 Gao, B., Huang, T., Ju, X., Gu, B., Huang, W., Xu, L., … Cui, S. (2018). Chinese cropping
602 systems are a net source of greenhouse gases despite soil carbon sequestration. *Global*
603 *Change Biology*, *24*(12), 5590-5606. https://doi.org/10.1111/gcb.14425
604 Gao, S., Chang, D., Zou, C., Cao, W., Gao, J., Huang, J., … Thorup-Kristensen, K. (2018).
605 Archaea are the predominant and responsive ammonia oxidizing prokaryotes in a red
606 paddy soil receiving green manures. *European Journal of Soil Biology*, *88*, 27–35.

https://doi.org/https://doi.org/10.1016/j.ejsobi.2018.05.008

Gerber, J. S., Carlson, K. M., Makowski, D., Mueller, N. D., Garcia de Corstazar-Atauri, I., Havlík, P., … West, P. C. (2016). Spatially explicit estimates of N_2O emissions from croplands suggest climate mitigation opportunities from improved fertilizer management. *Global Change Biology*, *22*(10), 3383–3394. https://doi.org/10.1111/gcb.13341

Guan, D., Meng, J., Reiner, D. M., Zhang, N., Shan, Y., Mi, Z., … Davis, S. J. (2018). Structural decline in China's CO_2 emissions through transitions in industry and energy systems. *Nature Geoscience*, *11*(8), 551–555. https://doi.org/10.1038/s41561-018-0161-1

International Fertilizer Association (IFA). IFA database. Retrieved June 18, 2018, from http://ifadata.fertilizer.org/ucSearch.aspx

IPCC. (2006). *Guidelines for National Greenhouse Gas Inventories*. https://doi.org/http://www.ipcc-nggip.iges.or.jp/public/2006gl/pdf/2_Volume2/V2_3_Ch3_Mobile_Combustion.pdf

Ito, A., & Inatomi, M. (2012). Use of a process-based model for assessing the methane budgets of global terrestrial ecosystems and evaluation of uncertainty. *Biogeosciences*, *9*(2), 759–773. https://doi.org/10.5194/bg-9-759-2012

Jäger, N., Stange, C. F., Ludwig, B., & Flessa, H. (2011). Emission rates of N_2O and CO_2 from soils with different organic matter content from three long-term fertilization experiments—a laboratory study. *Biology and Fertility of Soils*, *47*(5), 483. https://doi.org/10.1007/s00374-011-0553-5

Janssens-Maenhout, G., Crippa, M., Guizzardi, D., Muntean, M., Schaaf, E., Dentener, F., … Petrescu, A. M. R. (2017). EDGAR v4.3.2 Global Atlas of the three major Greenhouse Gas Emissions for the period 1970–2012. *Earth System Science Data Discussions*. https://doi.org/10.5194/essd-2017-79

632 Jiang, C., Lu, D., Zu, C., Shen, J., Wang, S., Guo, Z., … Wang, H. (2018). One-time root-zone
633 N fertilization increases maize yield, NUE and reduces soil N losses in lime concretion
634 black soil. *Scientific Reports*, *8*(1), 10258. https://doi.org/10.1038/s41598-018-28642-0
635 Li, C., Zhuang, Y., Cao, M., Crill, P., Dai, Z., Frolking, S., ... & Wang, X. (2001). Comparing
636 a process-based agro-ecosystem model to the IPCC methodology for developing a
637 national inventory of N_2O emissions from arable lands in China. *Nutrient Cycling in*
638 *Agroecosystems*, *60*(1-3), 159-175. https://doi.org/10.1023/A:101264220
639 Liu, J., Kuang, W., Zhang, Z., Xu, X., Qin, Y., Ning, J., … Chi, W. (2014). Spatiotemporal
640 characteristics, patterns and causes of land use changes in China since the late 1980s. *Acta*
641 *Geographica Sinica*, *69*(1), 3–14. https://doi.org/10.11821/dlxb201401001
642 Lu, C., & Tian, H. (2017). Global nitrogen and phosphorus fertilizer use for agriculture
643 production in the past half century: Shifted hot spots and nutrient imbalance. *Earth System*
644 *Science Data*, *9*(1), 181–192. https://doi.org/10.5194/essd-9-181-2017
645 Ma, L., Shan, J., & Yan, X. (2015). Nitrite behavior accounts for the nitrous oxide peaks
646 following fertilization in a fluvo-aquic soil. *Biology and Fertility of Soils*, *51*(5), 563–572.
647 https://doi.org/10.1007/s00374-015-1001-8
648 Ministry of Agriculture of the People's Republic of China. *Regional Planning of Advantageous*
649 *Agricultural Products (2003-2007)*. Retrieved March 18, 2018, from
650 http://www.moa.gov.cn/ztzl/ysncpqybjgh/200302/t20030212_54322.htm
651 Myhre, G., Shindell, D., Breon, F.-M., Collins, W., Fuglestvedt, J., Huang, J., … Zhang, H.
652 (2013). Anthropogenic and Natural Radiative Forcing. In: Stocker, T. F., D. Qin, G.-K.
653 Plattner, M. Tignor, S. K. Allen, J. Boschung, A. Nauels, Y. Xia, V. Bex & P. M. Midgley
654 (eds.), Climate Change 2013: The Physical Science Basis. Contribution of Working Group
655 I to the Fifth Assessment Report of the Intergovernmental Panel on Climate Change.
656 Cambridge University Press, Cambridge, United Kingdom and New York, NY, USA,

1535 pp, doi:10.1017/CBO9781107415324.

National Development and Reform Commission (NDRC). *China's National Climate Change Program*. Retrieved March 18, 2018, from http://www.china-un.org/eng/gyzg/t626117.htm

Paustian, K., Lehmann, J., Ogle, S., Reay, D., Robertson, G. P., & Smith, P. (2016). Climate-smart soils. *Nature*, *532*(7597), 49–57. https://doi.org/10.1038/nature17174

Perlman, J., Hijmans, R. J., & Horwath, W. R. (2014). A metamodelling approach to estimate global N_2O emissions from agricultural soils. *Global Ecology and Biogeography*, *23*(8), 912–924. https://doi.org/10.1111/geb.12166

Pettitt, A. N. (1979). A Non-Parametric Approach to the Change-Point Problem. *Applied Statistics*, *28*(2), 126–135. https://doi.org/10.2307/2346729

Philibert, A., Loyce, C., & Makowski, D. (2012). Quantifying Uncertainties in N_2O Emission Due to N Fertilizer Application in Cultivated Areas. *PLoS ONE*, *7*(11), e50950. https://doi.org/10.1371/journal.pone.0050950

Ravishankara, A. R., Daniel, J. S., & Portmann, R. W. (2009). Nitrous oxide (N_2O): The dominant ozone-depleting substance emitted in the 21st century. *Science*, *326*(5949), 123–125. https://doi.org/10.1126/science.1176985

Richards, M., Butterbach-Bahl, K., Jat, M. L., Ortiz-Monasterio, I., Sapkota, T., & Lipinski, B. (2015). *Site-Specific Nutrient Management: Implementation guidance for policymakers and investors*. https://doi.org/10.1177/002204269702700108

Saikawa, E., Prinn, R. G., Dlugokencky, E., Ishijima, K., Dutton, G. S., Hall, B. D., … Elkins, J. W. (2014). Global and regional emissions estimates for N_2O. *Atmospheric Chemistry and Physics*, *14*(9), 4617–4641. https://doi.org/10.5194/acp-14-4617-2014

Sandor, R., Ehrhardt, F., Brilli, L., Carozzi, M., Recous, S., Smith, P., … Bellocchi, G. (2018). The use of biogeochemical models to evaluate mitigation of greenhouse gas emissions

682 from managed grasslands. *Science of the Total Environment*, *642*, 292-306.
683 https://doi.org/10.1016/j.scitotenv.2018.06.020
684 Shcherbak, I., Millar, N., & Robertson, G. P. (2014). Global metaanalysis of the nonlinear
685 response of soil nitrous oxide (N_2O) emissions to fertilizer nitrogen. *Proceedings of the*
686 *National Academy of Sciences*, *111*(25), 9199–9204.
687 https://doi.org/10.1073/pnas.1322434111
688 Song, X., Liu, M., Ju, X., Gao, B., Su, F., Chen, X. & Rees, R. M. (2018). Nitrous oxide
689 emissions increase exponentially when optimum nitrogen fertilizer rates are exceeded in
690 the North China Plain. *Environmental Science & Technology*, *52*(21), 12504-12513.
691 https://doi.org/10.1021/acs.est.8b03931
692 Sun, W., & Huang, Y. (2012). Synthetic fertilizer management for China's cereal crops has
693 reduced N_2O emissions since the early 2000s. *Environmental Pollution*, *160*, 24–27.
694 https://doi.org/10.1016/j.envpol.2011.09.006
695 The National Development and Reform Commission. *The People's Republic of China National*
696 *Greenhouse Gas Inventory in 2005*. China Environmental Science Press.
697 Tian, H., Chen, G., Lu, C., Xu, X., Hayes, D. J., Ren, W., … Wofsy, S. C. (2015). North
698 American terrestrial CO_2 uptake largely offset by CH_4 and N_2O emissions: toward a full
699 accounting of the greenhouse gas budget. *Climatic Change*, *129*(3–4), 413–426.
700 https://doi.org/10.1007/s10584-014-1072-9
701 Tian, H., Lu, C., Ciais, P., Michalak, A. M., Canadell, J. G., Saikawa, E., … Wofsy, S. C.
702 (2016). The terrestrial biosphere as a net source of greenhouse gases to the atmosphere.
703 *Nature*, *531*(7593), 225–228. https://doi.org/10.1038/nature16946
704 Tian, H., Yang, J., Lu, C., Xu, R., Canadell, J. G., Jackson, R. B., … Zhu, Q. (2018). The
705 Global N_2O Model Intercomparison Project. *Bulletin of the American Meteorological*
706 *Society*, *99*(6), 1231–1251. https://doi.org/10.1175/BAMS-D-17-0212.1

Tian, H., Yang, J., Xu, R., Lu, C., Canadell, J. G., Davidson, E. A., ... & Gerber, S. (2019). Global soil nitrous oxide emissions since the preindustrial era estimated by an ensemble of terrestrial biosphere models: Magnitude, attribution, and uncertainty. *Global Change Biology*, *25*(2), 640-659. https://doi.org/10.1111/gcb.14514

USEPA (2012). *Global Anthropogenic Non-CO_2 Greenhouse Gas Emissions : 1990 - 2030. Office of Atmospheric Programs Climate Change Division U.S. Environmental Protection Agency*. https://doi.org/EPA 430-R-12-006

Van Drecht, G., Bouwman, A. F., Knoop, J. M., Beusen, A. H. W., & Meinardi, C. R. (2003). Global modeling of the fate of nitrogen from point and nonpoint sources in soils, groundwater, and surface water. *Global Biogeochemical Cycles*, *17*(4), 1115. https://doi.org/10.1029/2003GB002060

Vet, R., Artz, R. S., Carou, S., Shaw, M., Ro, C. U., Aas, W., … Reid, N. W. (2014). A global assessment of precipitation chemistry and deposition of sulfur, nitrogen, sea salt, base cations, organic acids, acidity and pH, and phosphorus. *Atmospheric Environment*, *93*, 3–100. https://doi.org/10.1016/j.atmosenv.2013.10.060

Wang, R., Goll, D., Balkanski, Y., Hauglustaine, D., Boucher, O., Ciais, P., … Tao, S. (2017). Global forest carbon uptake due to nitrogen and phosphorus deposition from 1850 to 2100. *Global Change Biology*, *23*(11), 4854–4872. https://doi.org/10.1111/gcb.13766

Wang, S., Luo, S., Li, X., Yue, S., Shen, Y., & Li, S. (2016). Effect of split application of nitrogen on nitrous oxide emissions from plastic mulching maize in the semiarid Loess Plateau. *Agriculture, Ecosystems and Environment*, *220*, 21–27. https://doi.org/10.1016/j.agee.2015.12.030

Winiwarter, W., Höglund-Isaksson, L., Klimont, Z., Schöpp, W., & Amann, M. (2018). Technical opportunities to reduce global anthropogenic emissions of nitrous oxide. *Environmental Research Letters*, *13*(1), 014011. https://doi.org/10.1088/1748-

9326/aa9ec9

Xia, L., Lam, S. K., Wolf, B., Kiese, R., Chen, D., & Butterbach-Bahl, K. (2018). Trade-offs between soil carbon sequestration and reactive nitrogen losses under straw return in global agroecosystems. *Global Change Biology*, *24*(12), 5919–5932. https://doi.org/10.1111/gcb.14466

Yue, Q., Cheng, K., Ogle, S., Hillier, J., Smith, P., Abdalla, M., ... & Pan, G. (2019). Evaluation of four modelling approaches to estimate nitrous oxide emissions in China's cropland. *Science of the Total Environment*, *652*, 1279-1289. https://doi.org/10.1016/j.scitotenv.2018.10.336

Yue, Q., Ledo, A., Cheng, K., Albanito, F., Lebender, U., Sapkota, T. B., ... & Pan, G. (2018). Re-assessing nitrous oxide emissions from croplands across Mainland China. *Agriculture, Ecosystems and Environment*, *268*, 70-78. https://doi.org/10.1016/j.agee.2018.09.003

Zaehle, S., & Friend, A. D. (2010). Carbon and nitrogen cycle dynamics in the O-CN land surface model: 1. Model description, site-scale evaluation, and sensitivity to parameter estimates. *Global Biogeochemical Cycles*, *24*(1), GB1005. https://doi.org/10.1029/2009GB003521

Zhang, B., Tian, H., Lu, C., Dangal, S. R. S., Yang, J., & Pan, S. (2017). Global manure nitrogen production and application in cropland during 1860-2014: A 5 arcmin gridded global dataset for Earth system modeling. *Earth System Science Data*, *9*(2), 667–678. https://doi.org/10.5194/essd-9-667-2017

Zhang, Y. L., Fan, J. B., Wang, D. S., & Shen, Q. R. (2009). Genotypic Differences in Grain Yield and Physiological Nitrogen Use Efficiency Among Rice Cultivars. *Pedosphere*, *19*(6), 681–691. https://doi.org/10.1016/S1002-0160(09)60163-6

Zhou, F., Shang, Z., Ciais, P., Tao, S., Piao, S., Raymond, P., ... & Peng, S. (2014). A new high-resolution N_2O emission inventory for China in 2008. *Environmental science &*

technology, *48*(15), 8538-8547. https://doi.org/10.1021/es5018027

Zhou, F., Shang, Z., Zeng, Z., Piao, S., Ciais, P., Raymond, P. A., … Mao, Q. (2015). New model for capturing the variations of fertilizer-induced emission factors of N_2O. *Global Biogeochemical Cycles*, *29*(6), 885–897. https://doi.org/10.1002/2014GB005046

Zhu, X., Li, Y., Li, M., Pan, Y., & Shi, P. (2013). Agricultural irrigation in China. *Journal of Soil and Water Conservation*, *68*(6), 147–154. https://doi.org/10.2489/jswc.68.6.147A

Zou, J., Lu, Y., & Huang, Y. (2010). Estimates of synthetic fertilizer N-induced direct nitrous oxide emission from Chinese croplands during 1980–2000. *Environmental Pollution*, *158*(2), 631-635. https://doi.org/10.1016/j.envpol.2009.08.026

Zuo, L., Zhang, Z., Carlson, K. M., MacDonald, G. K., Brauman, K. A., Liu, Y., ... & Wang, X. (2018). Progress towards sustainable intensification in China challenged by land-use change. *Nature Sustainability*, *1*(6), 304-313. https://doi.org/10.1038/s41893-018-0076-2